Physical Property Measurements at the Geological Survey of Canada Paleomagnetism and Petrophysics Laboratory

Enkin, R.J.[1]

1. Geological Survey of Canada - Pacific, PO Box 6000, Sidney, BC V8L 4B2

ABSTRACT

Physical properties measurements for mineral exploration purposes require many specialized methods. The Geological Survey of Canada Paleomagnetism and Petrophysics Laboratory has developed practical solutions to optimize measurements of density and porosity, magnetic susceptibility and remanence, and electrical resistivity and chargeability on samples chosen for mineral exploration studies. These methods are outlined and general observations are offered, to help guide other labs in making useful high quality measurements.

1. INTRODUCTION

Measurement of the physical properties of rocks provides the link between the two dominant activities in mineral exploration: geological mapping and geophysical surveys. Geological mapping reveals the distribution of rocks and their alteration zones on the surface and in drill cores. Geophysical surveys locate the 3-dimensional distribution of physical properties, which are proxies for the ore bodies, their host lithologies and their cover. Gravity surveys depend on contrasts in density. Magnetic surveys image variations in magnetic susceptibility and remanence. A wide range of electrical and electromagnetic methods locate rocks of different electrical resistivity and chargeability.

To identify the geological sources of geophysical anomalies it is necessary to ascertain the physical property fingerprints of each rock type and each formation. It is also useful to compile a physical properties database to address several issues. For example, what are the spatial variations of both mean values and their dispersions? How do alteration processes modify physical properties and how can this information be exploited to provide vectors to economic deposits? Where are the geophysically imageable contrasts? What techniques should be applied to optimize geophysical surveys and their interpretation?

The Geological Survey of Canada - Pacific Division houses its Paleomagnetism and Petrophysics Laboratory (PPL) at the Pacific Geoscience Centre in Sidney, British Columbia. Physical properties of rocks measured in the PPL are reported as data spreadsheets (Enkin, et al., 2008) and incorporated in other data portals such as the Rock Property Database System hosted by Mira Geoscience http://rpds.mirageoscience.com/.

This document provides a brief description of the methods used in the PPL to measure density, magnetic properties and electric properties, and information helpful to the interpretation and application of the data it produces. There is particular emphasis on new methods and analysis techniques for electrical impedance spectra, in order to produce reliable measurements of electrical resistivity and chargeability. This paper, prepared for the workshop "Improving Exploration with Petrophysics: The Application of Magnetic Remanence and Other Rock Physical Properties to Geophysical Targeting" offered at the Exploration '17 conference in Toronto, October 2017, is an update of the GSC Open File 7227 (Enkin, et al., 2012).

2. SAMPLES

Most samples analyzed in the PPL are hand samples or pieces of exploration core submitted by collaborating geologists. It is important to consider the location distribution of samples. Some regions have excellent coverage due to the availability of suitable outcrops and recent geological activity that led to the sampling. The sampling, however, is never uniform. Mappers generally do not collect samples on the basis of volumetric representation, but rather they attempt to sample the range of available rock types. Exotic occurrences will be selected whereas the host rocks will only occasionally induce additional sampling. Extra sampling is particularly frequent on altered or mineralized rocks, which are the main targets for geophysical surveys precisely because of their rarity. Friable or unconsolidated samples require alternative methods to measure most physical properties, and are often not collected. It is thus essential, when compiling spatial and lithological mean values, to consider the appropriate weighting for each sample and, furthermore, to recognize the incompleteness of the collections.

Along with the original identification, each sample is given a PPL number consisting of 2 letters corresponding to the Provincial or Territorial postal abbreviation (e.g., BC for British Columbia, NT for the Northwest Territories) and 5 digits assigned sequentially. An upcoming goal is to have the PPL samples and results entered into the Geological Survey of Canada Sample Management System (SMS), where they are assigned a "Curation Number" and an "SMS ID". The SMS provides the opportunity to link physical properties data to all other field and lab data associated with the sample. All samples are photographed before processing.

In order to get full value out of the database, every sample must also have its corresponding metadata, most importantly its location and lithology. Lithologies are difficult to summarize as the specific descriptors used for any suite of samples depends

on the geological context and the particular focus of the geologists concerned. Whatever information is submitted with the samples is included in the results spreadsheet as an unformatted text entry. It is important, however, to establish a restricted set of standard lithologies in order to organize the results. As a compromise in the continual tension between "lumping" and "splitting", we use two classification schemes. First, we apply the Geological Survey of Canada lithological scheme established for field mappers using the GanFeld system (Shimamura, et al., 2008). Second, we use the much more restricted Mira Geoscience "Master Lithology" classification scheme developed by their employee Sharon Parsons (Parsons, et al., 2009). Both schemes use a 3-level hierarchy, but whereas the GSC scheme attempts to capture the specific details of any field situation and is allowed to expand, the Mira Geoscience scheme is fixed at 126 distinct lithologies. No system is ideal for all applications, but we find the Mira Geoscience scheme allows for rapid, useful comparison of results from disparate sources of samples.

In the PPL, we use relatively small samples of about 10 cm^3 in the geometry designed for paleomagnetism. Such small samples have the advantages of requiring less material collected and stored, and allowing focused studies of variations across inhomogeneous rocks. On the other hand, such small samples may poorly represent the bulk properties of inhomogeneous rock, and particularly miss textural effects in coarse-grained rocks such as pegmatites.

Figure 1: Drilling 2.5 cm diameter subsample cores from a hand sample or exploration core.

A useful hand sample for physical properties work is dominantly unweathered, and at least 5 cm across its smallest dimension, in order to allow subsampling of representative rock. Core subsamples are drilled with a 2.5 cm diameter water-cooled diamond bit (Fig. 1), and cut to ~2.2 cm-long right-cylinders. Efforts are made to pick a representative sub-sample of the hand specimen and to avoid drilling through pre-existing planes of weakness in the rock. When possible, samples are drilled perpendicular to stratification or foliation in order to sample all minerals contained in the rock sample and thus provide a better understanding of the bulk properties. However, oriented samples are cored perpendicular to the oriented surface. With split NQ core (48 mm diameter), we find it effective to drill along the axis to produce a full-length partial-cylinder sample rather than perpendicular for a short full-cylinder samples, but both geometries provide useful data. For particular cases, rectangular prisms are cut to allow studies of anisotropy. Once the core sample has been cut to length, the flat ends are smoothed using a lapidary disk sander.

If necessary, density and magnetic susceptibility can be measured on a whole hand sample or on bags of unconsolidated grains.

3. DENSITY AND POROSITY

Table 1: Density and Porosity terms and symbols.

Term	Symbol	Formula
Dry Weight	W_D	
Saturated Weight	W_S	
Immersed Weight	W_I	
Water Density	ρ_W	
Grain Volume	V_G	$(W_D - W_I) / \rho_W$
Pore Volume	V_P	$(W_S - W_D) / \rho_W$
Bulk Sample Volume	V_B	$(W_S - W_I) / \rho_W$
Grain Density	ρ_G	$W_D / (W_D - W_I) * \rho_W$
Dry Bulk Density	ρ_B	$W_D / (W_S - W_I) * \rho_W$
Saturated Bulk Density	ρ_S	$W_S / (W_S - W_I) * \rho_W$
Water Porosity	P_W	$(W_S - W_D) / (W_S - W_I)$

Density, the mass per unit volume (g/cm^3), is the physical property which affects gravity surveys. Density provides the most direct proxy for the degree of mineralization as most ore minerals are significantly denser than the silicates which dominate unmineralized rocks (Fig. 2). Alteration and weathering influence porosity which reduces density.

There are various definitions of density which have different applications. We adapt the terminology and notation of Johnson and Olhoeft, 1984 (Table 1). The "Grain Density" (ρ_G) takes account of the rock independent of the porosity. It is most useful for constraining the mineralogy of a sample. The "Dry Bulk Density" (ρ_B) measures a rock with the porosity filled with air, while for the "Saturated Bulk Density" (ρ_S), the porosity is filled with water. This last density is the most useful for gravity modelling as most rock sits below the water table. In petrophysical databases, unspecified "Density" should usually be interpreted to mean "Saturated Bulk Density".

The "Dry Weight" (W_D) is measured using an analytical balance (to 0.1 mg). Freshly cut samples are left to dry for a day or more before this step, and preferably the samples are dried in an 80°C oven overnight to remove any residual water. A vacuum oven is available for special cases.

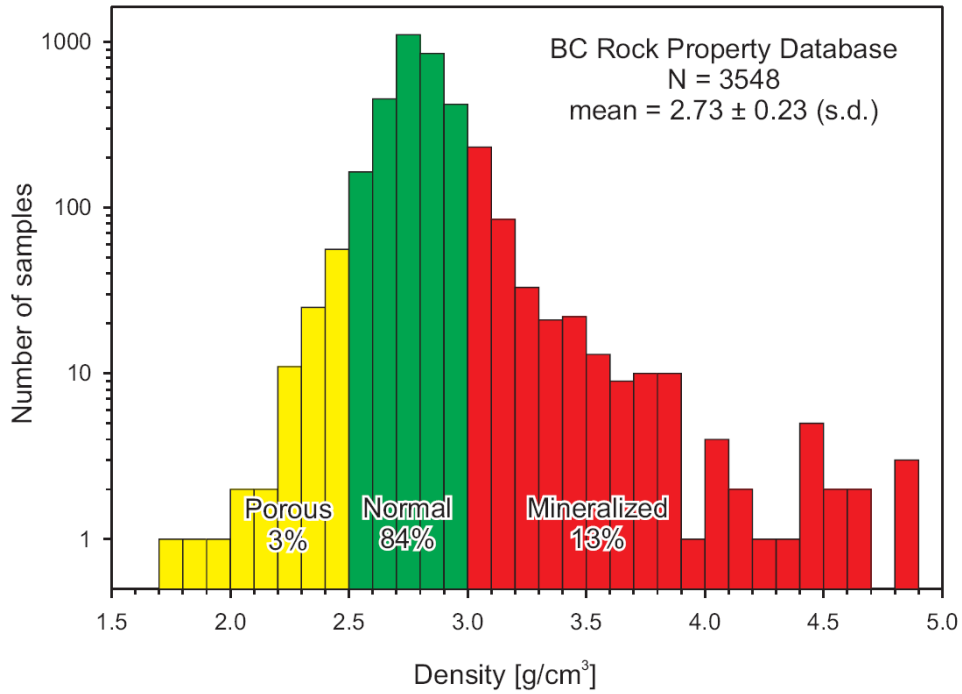

Figure 2: Density histogram from the British Columbia Rock Property Database

The "Grain Volume" (V_G), which excludes porosity, is measured using Archimedes method with water, or with a gas displacement pycnometer. The most accurate method to measure V_G involves destructively powdering the sample to ensure that the fluid used to measure the volume can access all porosity. As we are usually interested in maintaining the integrity of the samples, we accept that some porosity will not be connected to the outer sample surface and will not get filled.

The "Bulk Sample Volume" (V_B) which includes the pore space can be measured geometrically. The core diameter and length is measured with calipers (to 0.1 mm). Formulae for missing wedges or sides help estimate the volume of imperfect cylinders. The geometric volume is accurate to about 3% for typical samples around 10 cm^3 in volume, as long as the sample is sufficiently cylindrical. Unfortunately, such measurements are not nearly as accurate as methods using water impregnation, and we only use geometric bulk volume when samples fall apart on wetting.

The more accurate way to measure the volume V_B is by Archimedes' principle (weight in air - weight in water) using a specially built Jolly balance (Jolly, 1864). In order to completely saturate the samples with water, samples are placed in individual 100 mL beakers, 5 at a time, in a specially designed chamber (Fig. 3). Under vacuum (< 5 kPa) to void the rock pore space of as much gas as possible, the beakers are filled to 80 ml with distilled water. The chamber is placed on a shake table, to help the water work its way through necks in the permeable pathways. After bubbles stop streaming from the samples (about 3 minutes), the vacuum pump is turned off. We are experimenting with applying a sonicator to the water in the beakers to test if even more water can be imbibed into the porosity. Distilled water is used as part of the subsequent electrical measurements (see Section 5, below), and the samples sit in their beakers for 24 to 36 hours before the next measurements are done.

Each sample is removed from its beaker with metal tweezers and the outside is dried with lint-free paper, such as a KimWipe®. Tweezers are used to avoid affecting the electrical conductivity of the beaker water. It is important that the only water in the sample be contained within the pore space and not on the surface and that pore water is not removed via exposure or capillary action during the drying process.

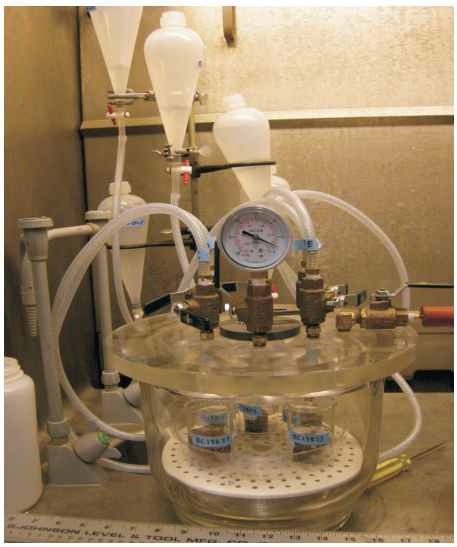

Figure 3: Chamber for vacuum impregnation of 5 subsamples.

Figure 4: The Immersed Weight (WI) of a sample being measured by suspension in a beaker of water below a balance, using a laboratory-designed Jolly balance.

The "Saturated Weight" (W_S) of the sample is measured on the pan of the analytical balance, and then the sample is suspended in a fine wire loop under the pan (Fig. 4). The sample's beaker with its original soaking water is lifted into place to immerse the sample, and the "Immersed Weight" (W_I) is measured. Note that the immersed mass also includes the buoyancy of the wire, requiring a small but near-constant correction.

The densities are calculated using the formulae in Table 1. On ~10 cm^3 samples, using a balance with 0.1 mg precision, the densities are precise to ±0.003 g/cm^3. The main source of error is the amount of residual water left on the sample before W_I is measured. The porosity $P_W = (V_B–V_G)/V_B$ is accurate to about ±0.2%.

4. MAGNETIC PROPERTIES

Magnetic survey anomalies arise from contrasts in the magnetization of rock bodies. The two magnetization mechanisms are induction (reversible magnetization when an external magnetic field such as the geomagnetic field is applied) and remanence (permanent magnetism acquired during the formation of the rock or during subsequent events such as hydrothermal alteration).

4a. Magnetic Susceptibility

Magnetic susceptibility (χ_0) is the per volume ratio of a rock's reversible magnetization to a small applied external magnetic field. While susceptibility is a dimensionless quantity, it is useful to think of the SI units of magnetic susceptibility as (A/m)/(A/m). Note that it is smaller in CGS units by an order of magnitude (precisely a factor 4π) because of a different set of equations used to describe magnetization and magnetic fields.

It is distressing how often published reports neglect to state the units of magnetic susceptibility, nor even the assumed power of 10. In the absence of units, one has to resort to a priori knowledge of reasonable magnetic susceptibility ranges (Fig. 5). Equant magnetite grains have a theoretical maximum magnetic susceptibility of 3 SI (Néel, 1955) and rock magnetic

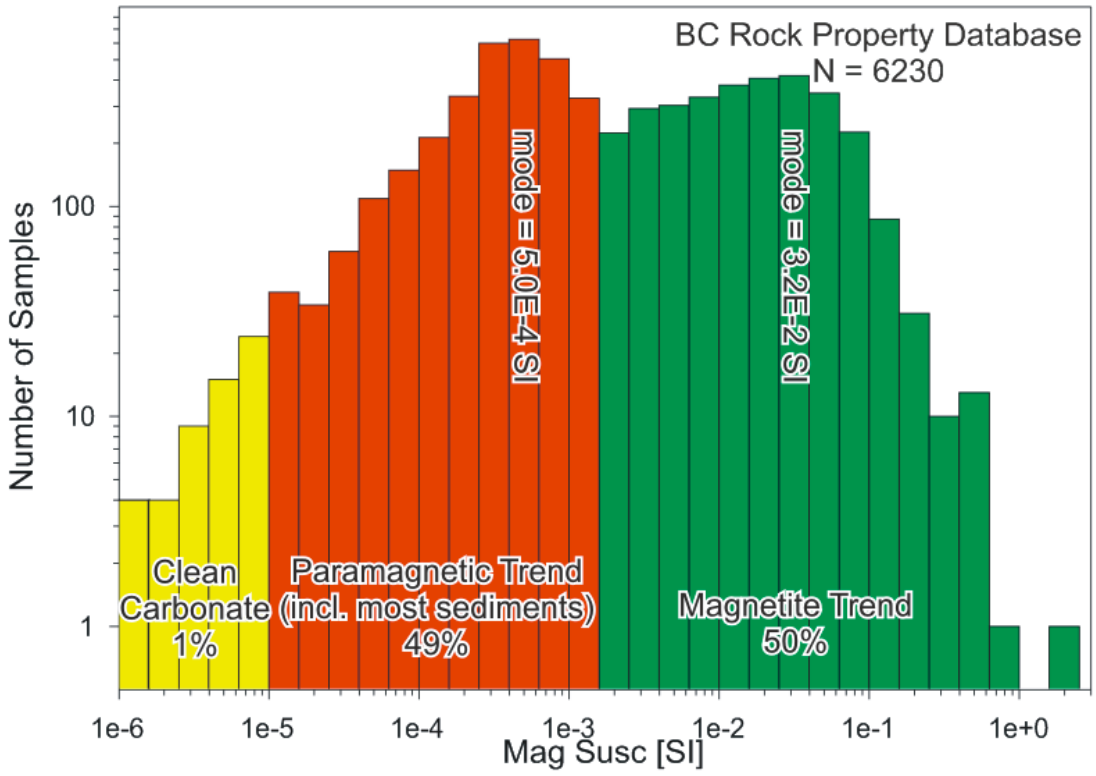

Figure 5: Magnetic susceptibility histogram from the British Columbia Rock Property Database.

Table 2: Magnetism terms and symbols.

Term	Symbol
Magnetic Susceptibility	χ_0
Natural Remanent Magnetization	NRM
Koenigsberger Ratio	K_N
Permeability of Free Space $4\pi\times10\text{-}7$ (A/m)/T	μ_0
Geomagnetic Field (A/m)	H_0
Geomagnetic Induction (T)	B_0
Induced Magnetism (A/m)	M_I
Remanent Magnetism (A/m)	M_R
Saturation Magnetism (A/m)	M_S
Remanence of Saturation (A/m)	M_{RS}
Coercive Force (T)	H_C
Remanent Coercive Force (T)	H_{CR}

measurements show that it is very rare to have susceptibilities above 5 SI (Heider, et al., 1996). Mafic rocks, which typically host a few percent magnetite by volume, usually have susceptibilities in the 10^{-2} SI range, while sediments and felsic rocks usually have susceptibilities in the 10^{-4} SI range. Pure quartz or carbonates are diamagnetic, that is they get magnetized antiparallel to the external field, but never with susceptibility larger than -15×10^{-6} SI. Small concentrations of clastic input often bring carbonate susceptibilities up to $+10^{-5}$ SI. Large negative susceptibilities are certainly contaminated by electric currents in electric conductors due to Faraday's law of induction. If a data table of magnetic susceptibilities does not fit these expected ranges, then the units must be suspected to have been incorrectly reported. In the PPL, magnetic susceptibilities are reported in per volume SI units.

Figure 6: GF Instruments SM20 Magnetic Susceptibility Meter.

The magnetic susceptibility of hand samples is measured with a GF Instruments SM20 magnetic susceptibility meter, distributed by ASC Scientific (Fig. 6). The unit, which operates at 10 kHz and has a 5 cm diameter coil, is ideal for field measurements. If a hand sample is less than 5 cm thick, then the observed susceptibility is low. Hand sample susceptibility is only reported in our summary tables when it is impossible to subsample, for example if the sample is too friable.

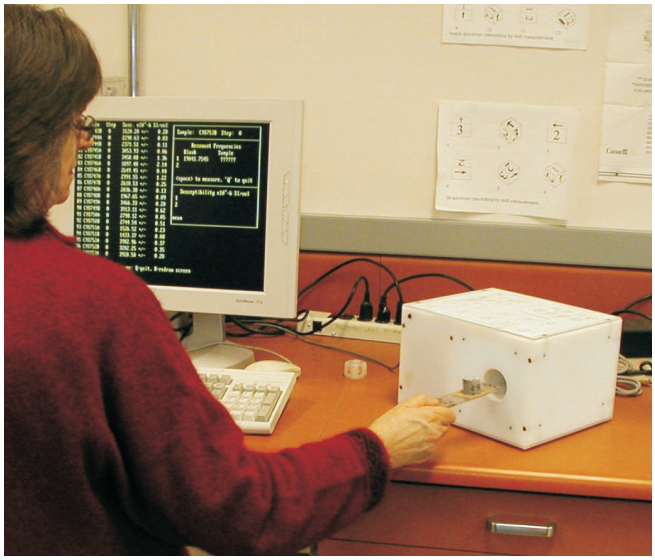

Figure 7: Sapphire Instruments SI2B Susceptibility Meter

Subsample cores are measured with a Sapphire Instruments SI2B susceptibility meter (Fig. 7). Its high operating frequency, 19.2 kHz, offers high sensitivity but has a smaller skin-depth in samples with high electrical conductivity. Thus it is important that samples are well dried before measurement. The SI2B is calibrated for an assumed volume of sample, so the values quoted are corrected for the true volume of the sample.

Note that magnetic susceptibility values are dominated by the concentrations of the minor accessory iron oxide and sulphide minerals, which vary significantly through an outcrop and even within a hand sample. Even though an individual measurement will have an uncertainty of better than 1%, natural variations of a factor 2 or 3 are expected on the cm-size scale, and order-of-magnitude variations are almost always observed across an outcrop.

The biplot of magnetic susceptibility against density almost always reveals two clusters, both showing magnetic susceptibility increasing with density, but one band with susceptibility between 10^{-4} and 10^{-3} SI, and the second between 10^{-2} and 10^{-1} SI (Fig. 8). This near-universal but rarely reported observation was discussed by Henkel (1991, 1994) who called the lower one the "paramagnetic trend" and the higher one the "magnetite trend".

4b. Magnetic Remanence and Koenigsberger Ratio

Magnetic anomalies are almost always interpreted as spatial variations in magnetic susceptibility, and the magnetic remanence is usually only considered when no reasonable

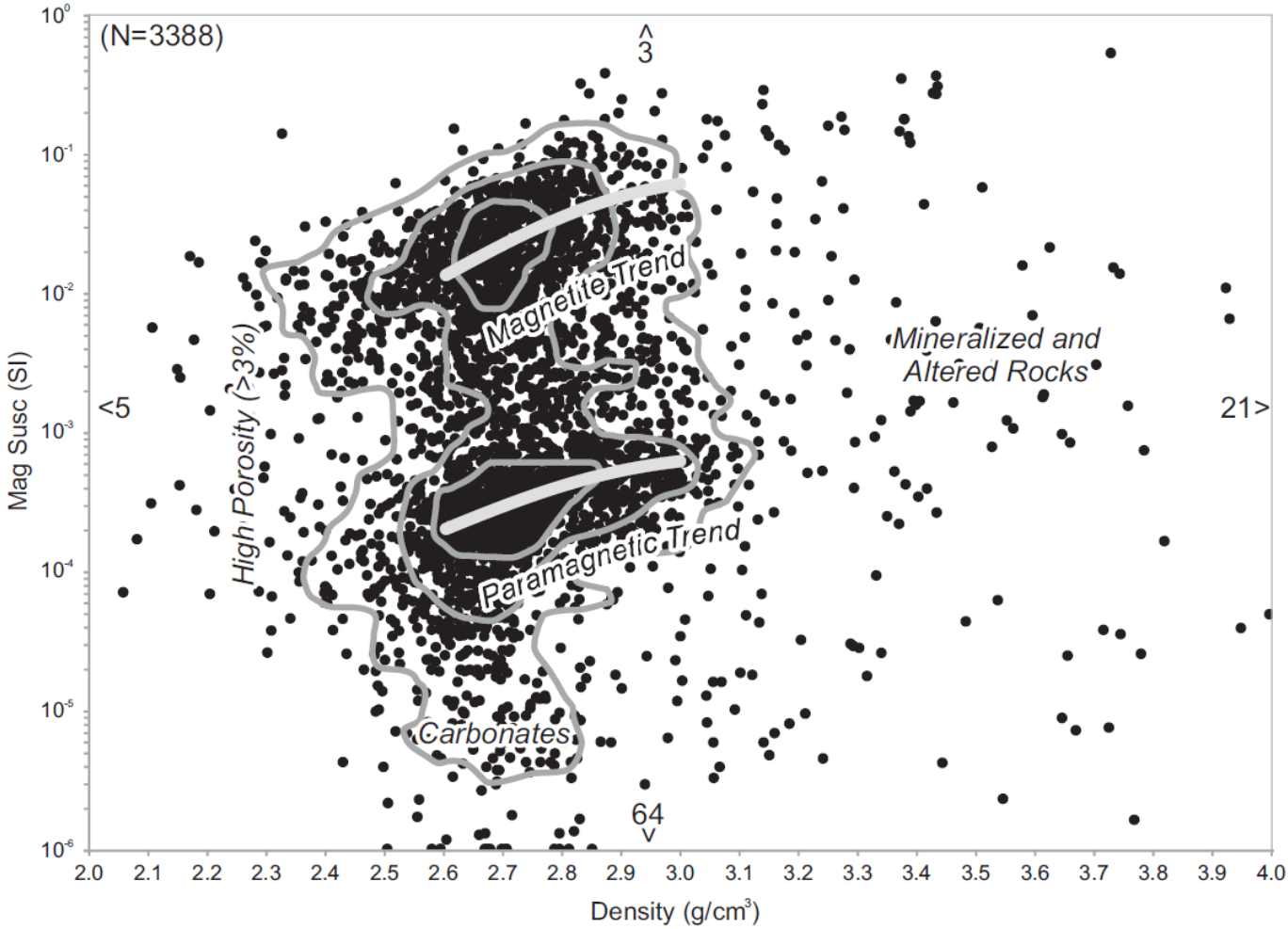

Figure 8: Density - magnetic susceptibility biplot from the British Columbia Rock Property Database

Figure 9: Agico JR5-A Spinner Magnetometer for measuring magnetic remanence.

interpretation can be proposed without it. Two notable examples of magnetic remanence dominating the magnetic surveys are the mid-oceanic stripes parallel to ocean ridges from where new crust spreads, and the point-like anomalies associated with kimberlite pipes. Whereas induced magnetization is nearly parallel to the external field, magnetic remanence can point in any direction.

The PPL is equipped to perform full paleomagnetic studies on collections of oriented rocks, with applications to paleogeography, deformation history, the dating of hydrothermal events, and magnetostratigraphic dating. For petrophysical work, it is useful to measure the magnitude of natural magnetic remanence (NRM) even for unoriented samples.

Magnetic remanence is measured on an Agico JR5-A spinner magnetometer (Fig. 9), using the standard cylindrical subsamples. The JR5-A has a sensitivity of 10^{-5} A/m. As with the susceptibility measurements, the remanence is corrected for the volume of the sample.

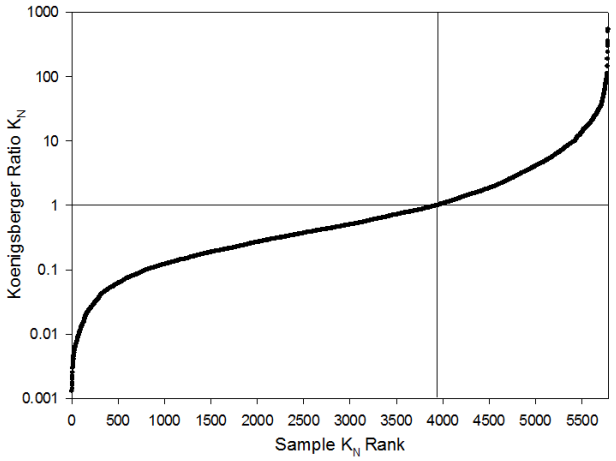

Figure 10: Koengsberger ratios from the Canadian Rock Physical Properties Database showing that ⅓ have $K_N>1$.

One important complication is that samples dominated with iron oxides, such as iron formations, can get magnetized during sampling. The effect can be highlighted by simply tapping the sample with a hammer and re-measuring to observe if there is change caused by piezomagnetic remanence. In such cases, a more realistic measure of the natural remanence is made by first performing a gentle alternating field demagnetization step of 2 mT maximum intensity. We use a Schonstedt GSD-5 alternating field demagnetizer with 2-axis tumbler.

The Koenigsberger ratio (K_N) is the natural remanent magnetization divided by the induced magnetization:

$$K_N = NRM / \chi_0 H_0 , \qquad [eq.1]$$

where $H_0 = B_0/\mu_0$ is the strength of the geomagnetic field. The units of H_0 are A/m, but the geomagnetic field strength is usually quoted as magnetic induction (B_0) with units of Tesla (T). The conversion factor is the permittivity of free space, $\mu_0 = 4\pi\times10^{-7}$ (A/m)/T. For comparing the efficiency of magnetization among different rocks, the Koenigsberger ratio is reported using a standard field of $B_0 = 50$ μT, however for more accurate magnetic anomaly interpretation, it is important to use the local geomagnetic field strength, which in Canada varies from 51 to 60 μT.

Most rocks have a Koenigsberger ratio below 1 (Fig. 10, 11). This observation is often used as justification for not including magnetic remanence in magnetic survey interpretations. Nevertheless, it is impossible to know how big the influence of

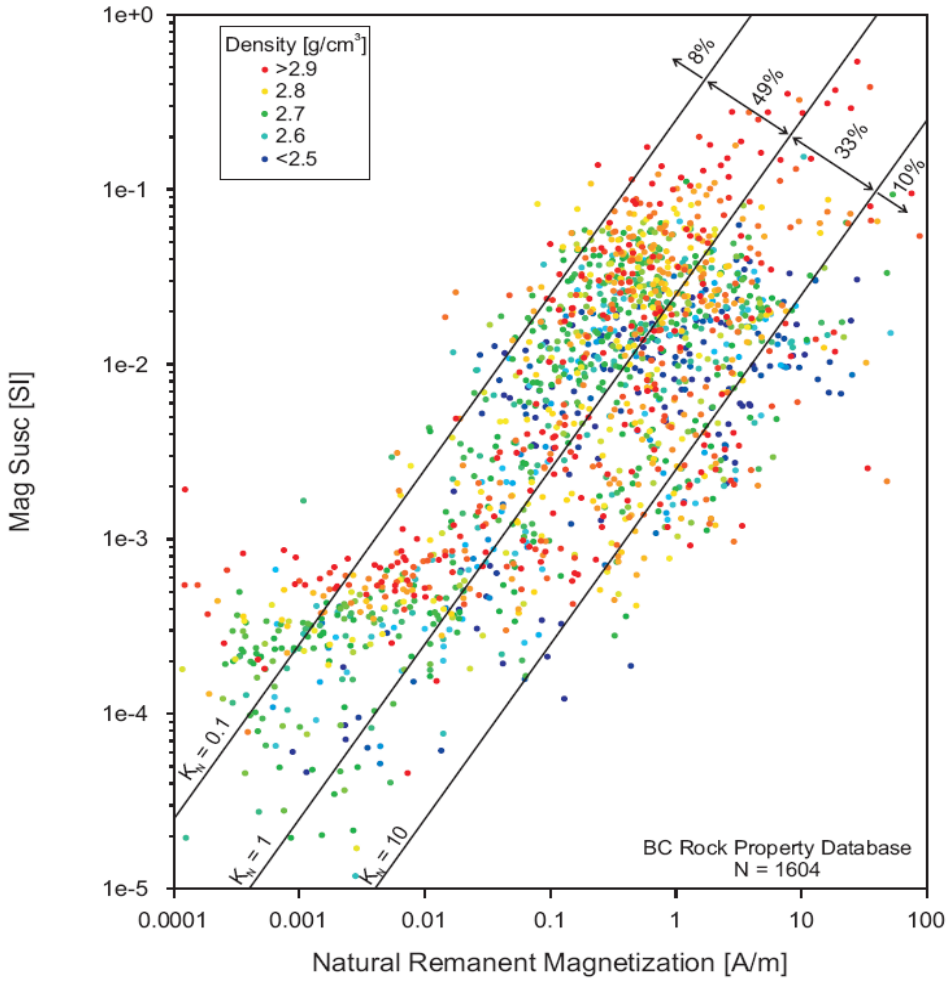

Figure 11: : Magnetic remanence - magnetic susceptibility biplot from the British Columbia Rock Property Database, displaying lines of equal Koenigsberger ratio. The colours display density variations.

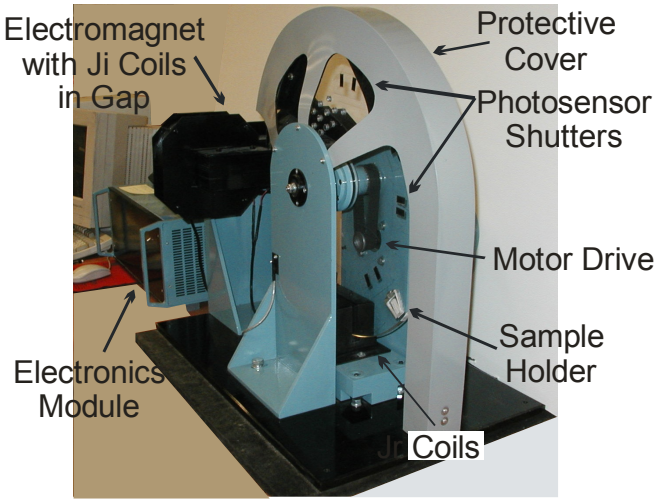

Figure 12: J-Meter Coercivity Spectrometer

remanence can be without measuring it on rock samples. Note that 32% of the samples we have measured in the PPL have K_N>1. When a significant proportion of rocks from a region display high Koenigsberger ratios, then magnetic remanence plays an important role.

4c. Rock Magnetism Measurements

Detailed rock magnetic measurements efficiently reveal useful information concerning the iron oxides and sulphides which record many aspects of a rock's geological history. In sedimentary rocks, different sedimentary sources have distinct magnetic minerals fingerprints. In mineralized rocks, magnetic mineralalogy is controlled by the oxygen fugacity of hydrothermal fluids. Rock magnetic studies are designed to determine the mineralogical compositions, grain sizes and concentrations of magnetic grains.

The J-Meter Coercivity Spectrometer (Fig. 12) is designed for studying ferromagnetic minerals contained in rocks and sediments by simultaneously measuring magnetic hysteresis cycles and isothermal remanence magnetization (IRM) curves (Enkin, et al., 2007). Rock chips (~1 to 2 g) are placed in a 7mm×10mm×22mm box and packed with cotton to immobilize them. The box is inserted in a sample holder on the edge of the 50 cm diameter acrylic disk of the coercivity spectrometer. The disk spins at 17.5 Hz through the pole pieces of an electromagnet. With each rotation the induced magnetism (M_I) of the sample is measured with secondary coils within the pole pieces, and the remanence (M_R) is measured by a set of coils placed in a mu-metal magnetic shield. The magnetic field is ramped slowly up to 500 mT, and then down to the opposite polarity, -500 mT, making virtually continuous recordings of the hysteresis cycle, $M_I(H)$, and the IRM acquisition and re-magnetization curves, $M_R(H)$. The sensitivity of the M_R channel of the J-Meter is about 10^{-3} A/m, while the sensitivity of the M_I channel is only about 10^{-1} A/m because of the impossibility of damping out vibrations in the electromagnet. Each run takes only about 6 minutes, making the J-Meter an extremely efficient method to study many samples.

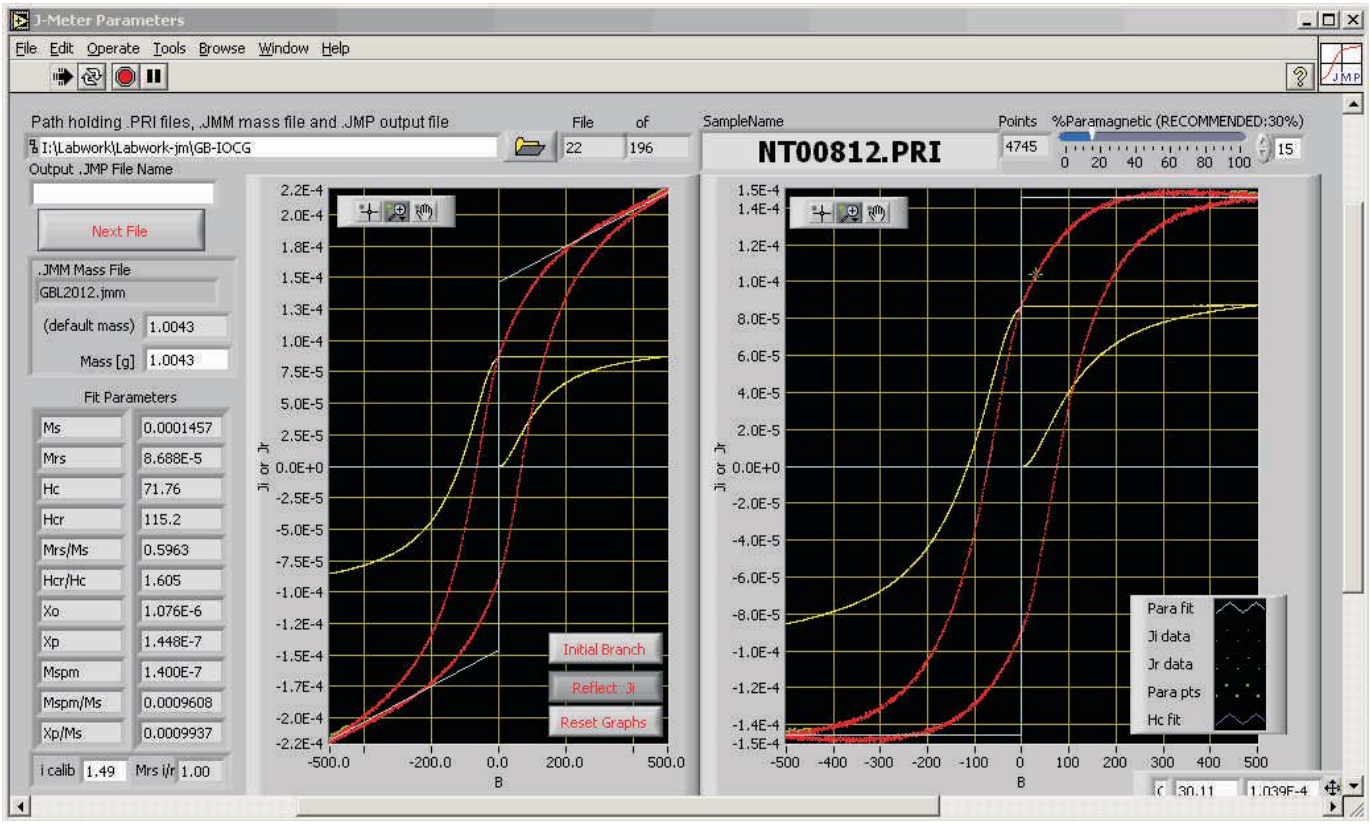

Figure 13: Screen-shot of LabView program JMP to analyze the J-Meter Coercivity Spectrometer output. The red trace marks the induced magnetization and the yellow trace marks the remanent magnetization. The left-hand graph displays the raw measurements, and the right hand graph has the paramagnetic susceptibility (blue lines) removed, revealing the ferromagnetic hysteresis curve.

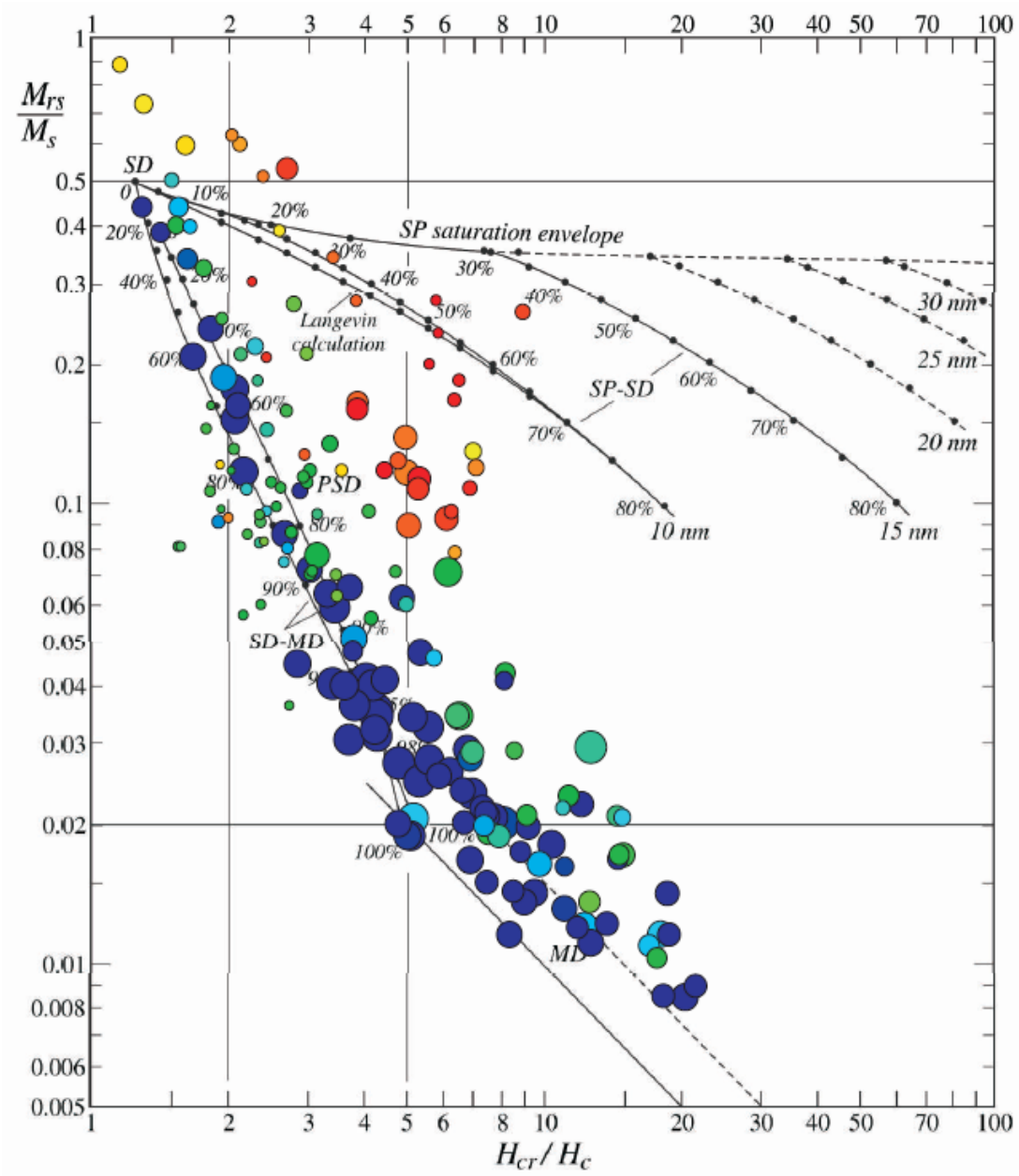

Figure 14: The Day plot (biplot of magnetic hysteresis ratios), on a base plot developed by Dunlop (2002) for titanomagnetite, of the Great Bear Iron Oxide Copper Gold (IOCG) database. The distribution displays a wide range of magnetic mineralogy, concentration and grain-size. The point size is proportional to the logarithm of the saturation magnetization (MS). The colour is from degree of high-field saturation, where blue marks complete saturation by 400 mT (typical of magnetite) and the hotter the colour the harder the magnetism. The yellows through reds are typical of hematite.

The LabView program JMP has been developed in-house to analyze the J-Meter output (Fig. 13). In particular, the standard hysteresis parameters of saturation magnetization (M_S), remanence of saturation (M_{RS}), coercive force (H_C), and the remanent coercive force (H_{CR}) are used to produce a Day plot (Day, et al., 1977; Dunlop, 2002) which helps specify the magnetic grain sizes in a sample (Fig. 14).

Curie temperatures of the magnetic minerals in a sample are determined by measuring the magnetic susceptibility as a function of temperature with a Bartington MS2WF thermomagnetic susceptibility meter (Fig. 15). Rock chips are placed in a crucible which sits within a furnace surrounded by a water-cooled susceptibility meter sensor. Magnetic susceptibility is monitored continuously as it is heated up to 700°C. Pyrrhotite is marked by a susceptibility drop between

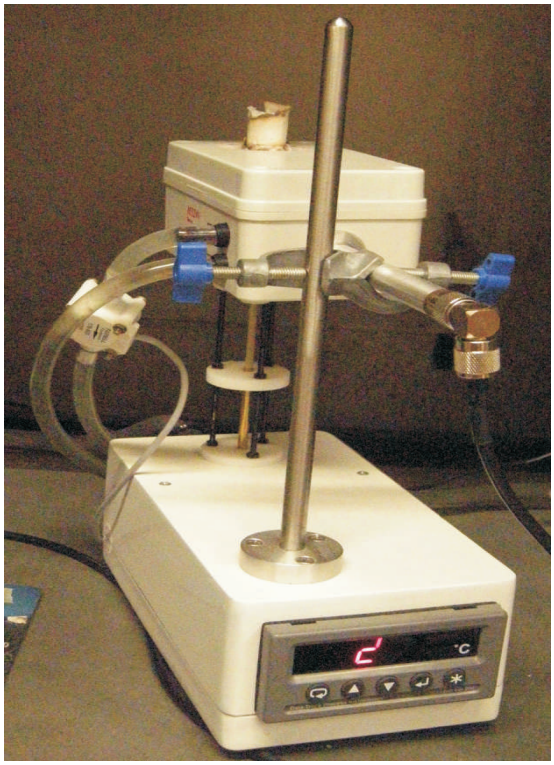

Figure 16: Bartington MS2WF Thermomagnetic Susceptibility Meter

300°C and 350°C, magnetite with a drop between 550°C and 580°C, and hematite by a drop above 650°C (Fig. 16).

Mineral alterations, such as oxidation of sulphides or reduction of hematite to magnetite are also observed during the heating and cooling of the samples. Together with the J-Meter, the Bartington MS2WF produces quantitative measurements of the magnetic mineralogy, grain size and concentration.

5. ELECTRICAL PROPERTIES

Electromagnetic (EM) surveys, including induced polarization (IP) and magnetotelluric (MT) methods, depend on how electric currents traverse through the ground. No physical property of Earth materials display as wide a range as electrical resistivity, from native copper and gold around 10^{-8} Ω·m to quartz around 10^{14} Ω·m. The critical issue is that the electrical properties are a function not only of the minerals that form the rocks, but also of the fluid pathways that traverse them.

For most rocks, the dominant mode of electrical conductivity is electrolytic conduction through ground water, following Archie's Law (Archie, 1942):

$$r = a P_W^{-m} S_W^{-n} r_W , \qquad \text{[eq.2]}$$

where the resistivity (r) is proportional to the ground-water resistivity (r_W), and to other terms describing the rock; a, a constant depending on rock type; porosity (P_W), the fraction of pore volume containing water (S_W); and two empirically determined exponents, m and n.

Since there usually is no possibility of recovering the ground

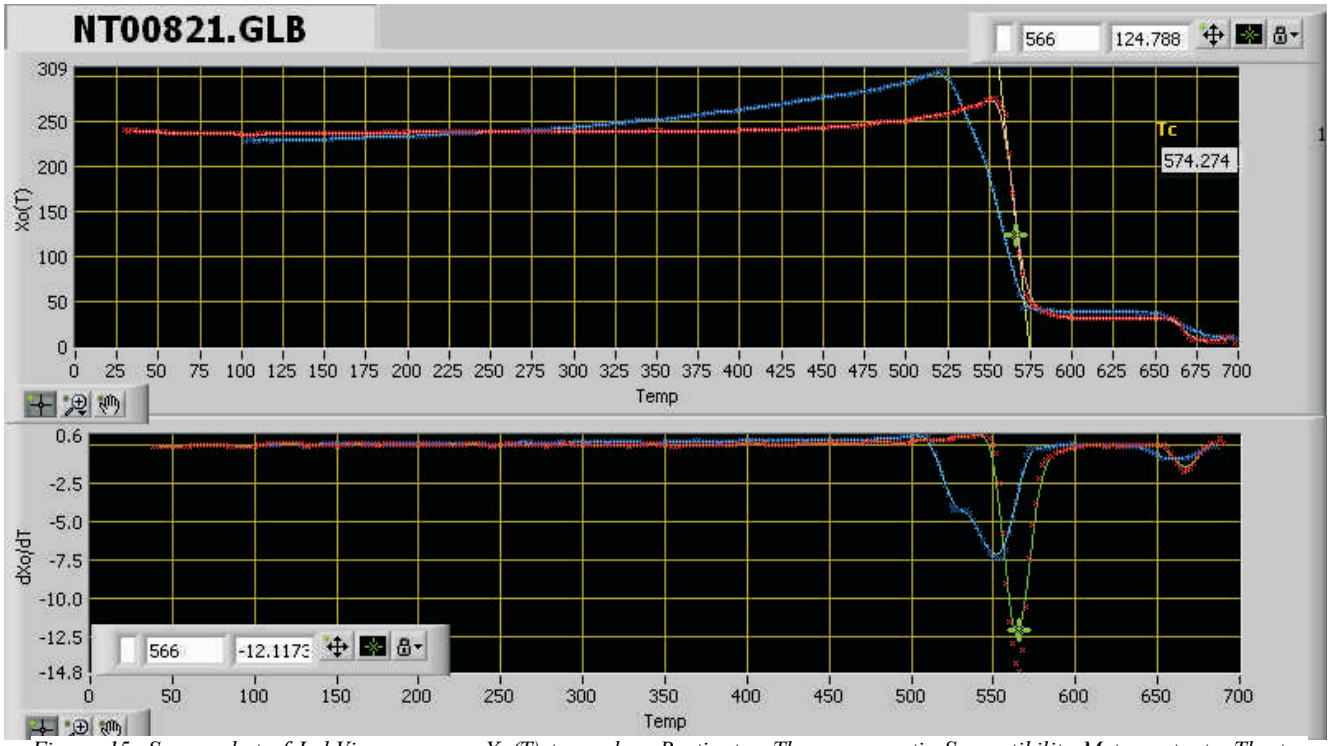

Figure 15: Screen-shot of LabView program Xo(T) to analyze Bartington Thermomagnetic Susceptibility Meter output. The top graph shows the magnetic susceptibility as a function of temperature during heating in red and during cooling in blue. The lower graph displays the time derivative of these curves. This sample contains both magnetite, with a Curie temperature of 570°C, and hematite, with a Curie temperature of 670°C.

Table 3: Electric terms and symbols.

Term	Symbol
Resistance (Ω)	R
Electrical Resistivity (Ωm)	ρ
Capacitance (F)	C
Electrical Impedance (Ω)	Z
Electrical Impedance Spectrum	EIS
Linear Frequency (Hz = s^{-1})	f
Angular Frequency [s^{-1}]	ω
Impedance of a Constant Phase Element (Ω)	Z_{CPE}
Initial Chargeability (mV/V)	M_0
Newmont Standard Chargeability (ms)	M_X

water with the rock samples, we approximate the original ground water through vacuum impregnation of the samples (Fig. 3) with deionized water (resistivity = 15 MΩ·cm) and let them sit for 24 to 36 hours. During this time, solutes, precipitated on pore walls when the sample originally dried, are dissolved into the water. Our measurements show that the resistivity of the water in the beaker reduces for days and weeks. However, the resistivity of the sample is close to stabilized after about 24 hours (Fig. 17). The interpretation is that the dissolution of the solutes within the pore spaces happens over hours, however, the diffusion of the solutes out of the sample is much slower.

Following vacuum impregnation and all the weighing procedures necessary for the density and porosity measurements (see Section 3, above), the cylindrical sample is patted dry with a KimWipe®. We use a sample holder (Fig. 18) consisting of two copper cylinders, the same diameter as the samples, designed to have a small and reproducible capacitance. With a 2.2 cm gap, the capacitance is 0.6 pF, increasing to about 4 pF with the sample in place depending on the dielectric constant of the rock and pore water. Rock contact is made through filter paper disks saturated with a $CuSO_4$ solution.

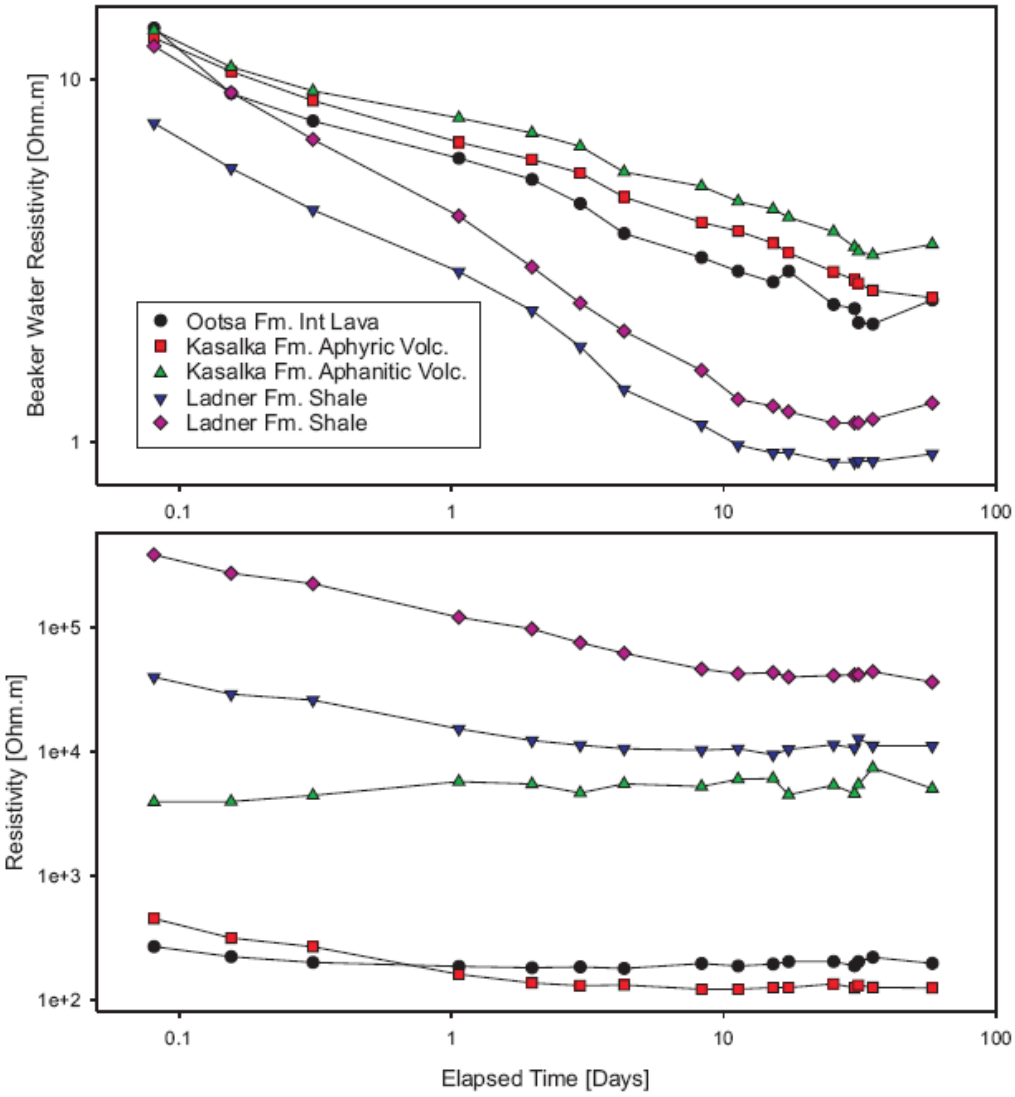

Figure 17: The time evolution of the resistivity of 5 rock samples and their immersion water. While the rock resistivity (bottom) usually stabilizes within a day or two, solutes continue to leach into the water for weeks.

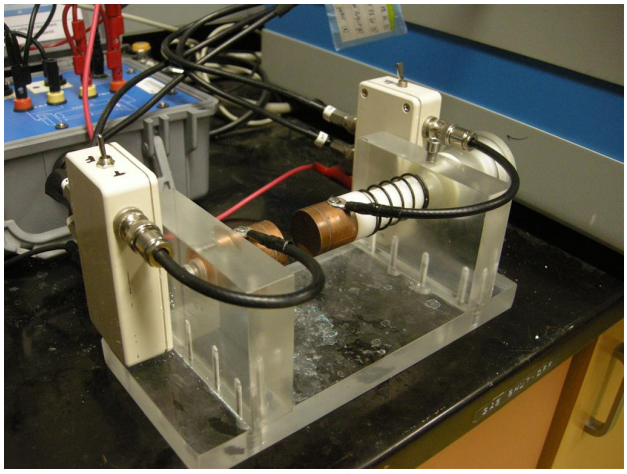

Figure 19: Electrode connections for rock electrical impedance measurements. The sample is placed in the gap between the copper electrodes with $CuSO_4$-saturated filter paper disks.

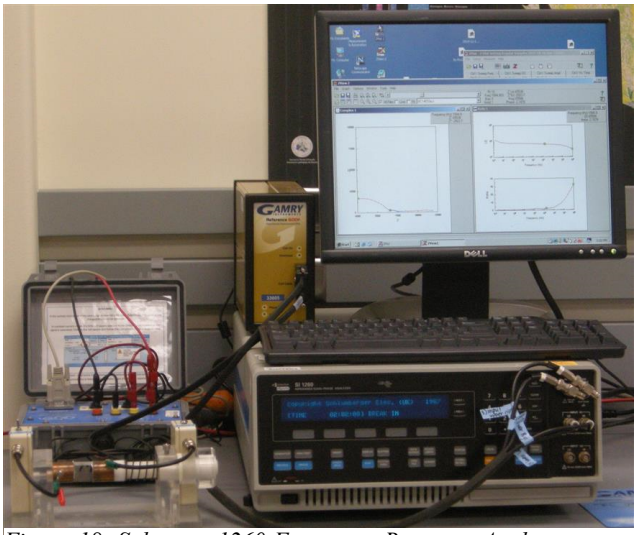

Figure 18: Solartron 1260 Frequency Response Analyzer set up to measure frequency domain electrical impedance. The GDD SCIP unit (behind sample holder) makes time-domain measurements, while the Gamry Reference 600+ can measure bith frequency domain and time domain impedance.

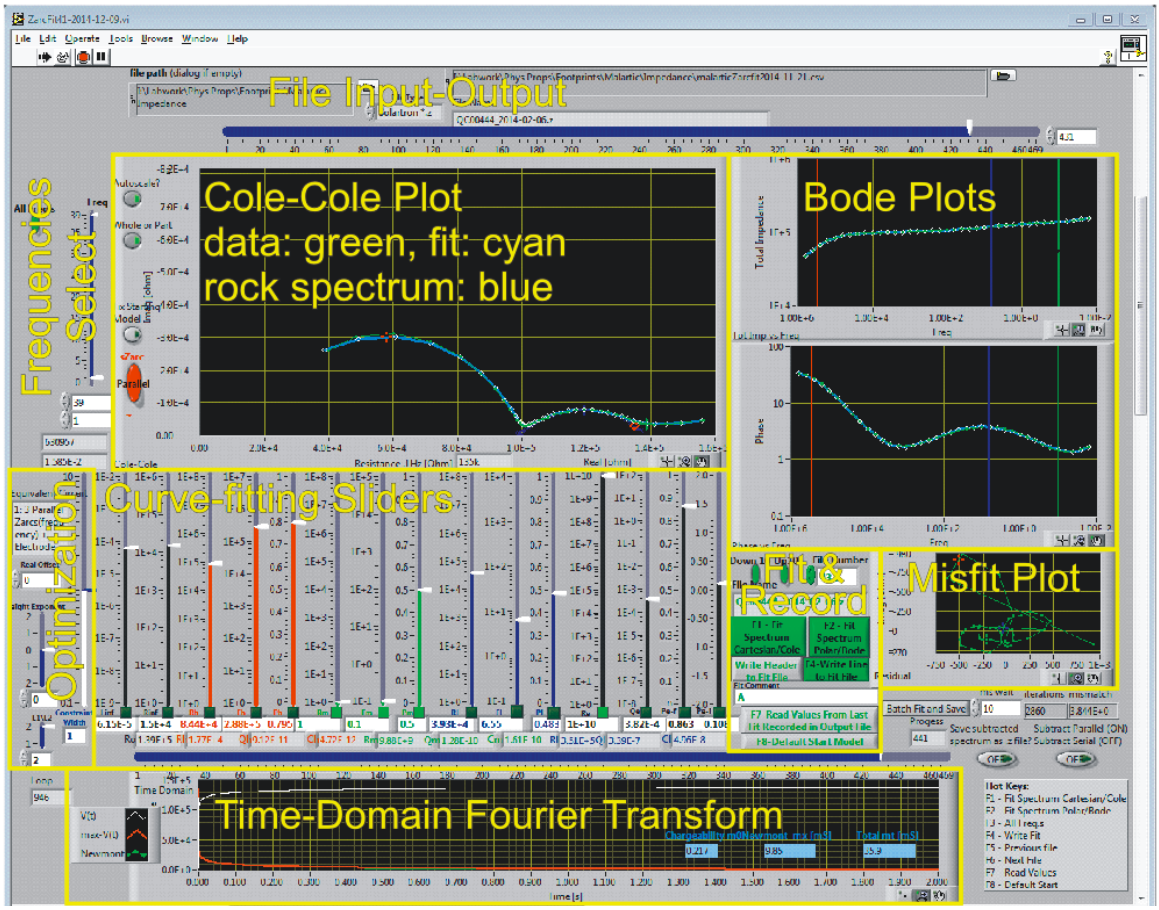

Figure 20: Screenshot of LabView program ZARCFIT for analysis of electrical impedance spectra.

Electrical impedance is a complex quantity; the real component of impedance is a measure of resistance or energy loss in a circuit, and the imaginary component of impedance is a measure of energy storage. An electrical impedance spectrum (EIS) is the frequency dependence of the complex impedance of a sample. The magnitude of the impedance is the ratio of the amplitude of the voltage drop across a sample and the current going through it. Its phase is the phase shift between these two quantities. In the PPL, we use a Solartron 1260 Frequency Response Analyzer to measure the impedance spectrum (Fig. 19). We have recently acquired a Gamry Reference 600+ Potentiostat, and are producing compatible results. The copper contacts are attached to the current and voltage inputs through grounded coaxial cables. The current is driven with a 1 V sinusoidal wave, at frequencies from 1 MHz down to 0.025 Hz (40 s period) at 5 frequencies each decade. Above 1 MHz, the sample has little influence on the spectrum while the effects of inductance and standing waves in the probes dominate. At very low frequencies, the dominant control is electrolyte diffusion across the electrode contacts.

The absolute value of the observed resistivity can vary by up to 50% depending on the state of the water. This uncertainty is insignificant as natural resistivities vary over many orders of magnitude and are plotted on logarithmic scales.

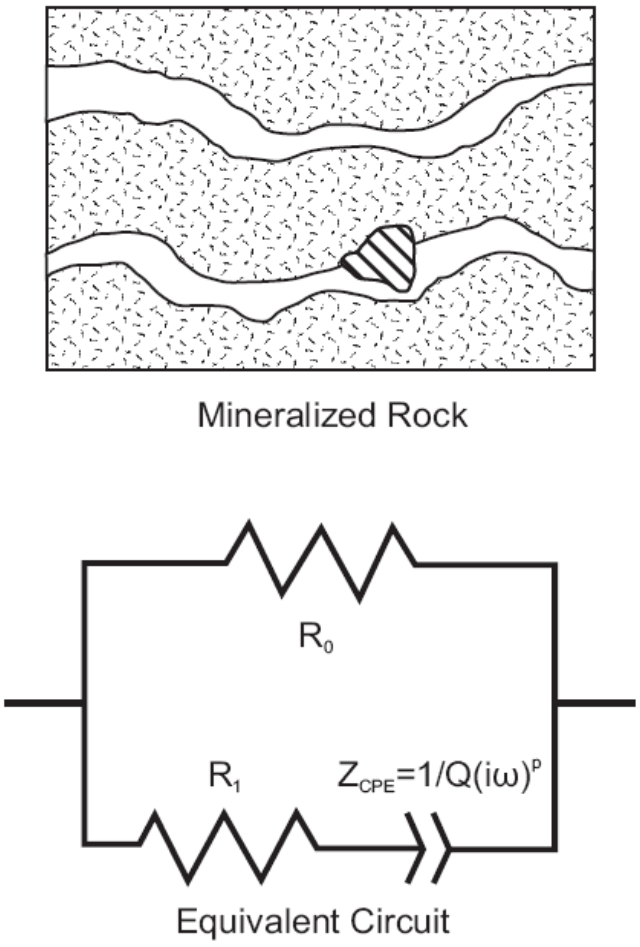

Figure 21: Simplified rock model and its equivalent circuit, after Pelton (1978)

New software (ZarcFit using LabView, Fig. 20) has been developed to model the electrical impedance spectrum in terms of equivalent circuits. The data is presented as both a Cole-Cole plot of the real and imaginary components of the impedance at each frequency (Cole and Cole, 1941), and as Bode plots of the impedance magnitude and phase as a function of frequency. The circuit response, with parameters set with a series of 15 sliders, is also plotted. Once a sufficiently close fit is made by hand, a simplex optimization algorithm minimizes a mismatch function (sum of square deviations) to determine best fit parameters.

Full documentation on how to operate and interpret the program is available from the PPL. Here are some important features:

The building blocks of the electrical impedance spectrum are "Zarcs", consisting of a parallel resistor and a constant phase element (Fig. 21). A constant phase element is a modified capacitor. A capacitor has the frequency response:

$$Z_C = 1 / Ci\omega \,, \qquad \text{[eq.3]}$$

where C is the capacitance, ω is the angular frequency ($\omega = 2\pi f$) and f is the linear frequency. The constant phase element has the frequency response:

$$Z_{CPE} = 1 / Q(i\omega)^p \,, \qquad \text{[eq.4]}$$

where p is an exponent and Q is the size of the constant phase element. If p=1, then $Z_{CPE} = Z_C$ (a capacitor). If p=0, then Z_{CPE} = R (a resistor). A Zarc on a Cole-Cole plot has the form of a sector of a circular arc with width equal to the resistance, and with a maximum at angular frequency

$$\omega_0 = (RQ)^{-1/p} \,. \qquad \text{[eq.5]}$$

The exponent p describes the spread in the relaxation times for the circuit element. If p=1, then the circuit has a single relaxation time $1/\omega_0$. The standard deviation of a log-normal distribution of relaxation times increases as p gets lower.

The EIS of most rocks can be described as a single high frequency Zarc, describing the Archie's law resistance and capacitance derived from the capacitance of the sample holder magnified by the dielectric constant of the sample and its pore water.

A low frequency Zarc response is common in rocks (Pelton et al., 1978), especially in mineralized samples (Fig. 20). The mechanism is storage of charge on the surfaces of electrically conductive grains (the electrode effect). This is the response being searched for using induced polarization (IP) techniques.

In interesting cases, we observe a triple-Zarc. We interpret the high frequency Zarc, Z_H (100s of kHz), to be due to the sample holder and the dielectric properties of the sample. The middle frequency Zarc, Z_M (100s to 1000s of Hz), to be due to "membrane chargeability" of ions interacting with clay mineral surfaces. The low frequency Zarc, Z_L (0.1s to 1s of Hz), to "electrode chargeability" at the interfaces between the ion transport through the permeability and conductive minerals.

Time-domain IP report survey results in terms of chargeability, which can be derived from the EIS equivalent circuit determined using ZarcFit. In an IP survey, electrical current is injected into the ground as a slow square-wave function. When the current is switched off, the voltage response is a decaying curve. Using the Newmont Standard, the chargeability (M_X) is

the area under the voltage curve from 430 to 1100 ms, normalized by the beginning voltage (units: ms). In ZarcFit, the sample's frequency response is converted into time domain by inverse Fourier transform and then numerically integrated (bottom of Fig. 20). An alternative definition, called initial chargeability (M_0), is usually defined as the instantaneous drop in voltage after the current is removed. In practical applications, current can never be stopped as a perfect step function, so the drop is measured at some short time after the current was shut down. There is high-frequency – short-duration storage of charge but it is too fast to be observed in a time domain IP measurement. For the determination of M_0 from the sample electrical impedance spectrum, we set the time for measuring the voltage drop to be 1 ms.

In series with the rock's equivalent circuit is the impedance of the apparatus, which must be fit and subtracted from the rock response before the resistance and chargeability are calculated. The apparatus effects are particularly observed at high and low frequencies. In theory, the resistance of the rock (R_0) should be the real impedance measured at zero frequency (direct current). Some labs choose the resistance at some arbitrary frequency, whereas others choose the resistance with the minimum phases shift in a frequency range. With ZarcFit, the apparatus and the rock impedance are simultaneously fit, allowing the rock spectrum to be reliably distinguished and separated.

Note that the extrinsic property of resistance is converted to the intrinsic property of resistivity by multiplying the sample resistance by the cross section area (A) and divide it by its length (l). The ratio A/l is called the geometric factor.

At high frequency (>100 kHz), and only observed in low resistivity rocks (R_0 < 10 kΩ), the inductance of the probe wires is seen as the impedance having positive imaginary values and positive phase shifts (i.e., inductance). This effect is modelled with a series inductor:

$$Z_L = Li\omega \qquad \text{[eq.6]}$$

At low frequency, there is the effect of diffusion across the electrodes. Theoretically, this type of impedance should have the form of a Warburg impedance:

$$Z_W = 1 / Q(i\omega)^{1/2} . \qquad \text{[eq.7]}$$

Empirically we find the low frequency electrode impedance is best described as a modified constant phase element:

$$Z_E = 1 / (Q_E\, i^{p_i} \omega^{p_f}) , \qquad \text{[eq.8]}$$

where p_i and p_f are separate exponents for the phase angle and the frequency. Interestingly, we observe that p_i can take any value between $\pm 2\pi$, but usually is close to either 0 or 2π signifying that low frequency impedance mostly affects real resistance rather than energy storage chargeability. It is important that the low-frequency electrode EIS be as accurately fit as possible, as it is extrapolated up to frequencies important for the determination of induced polarization chargeability.

Rocks naturally provide parallel conduction mechanisms, however the parameters which control a parallel circuit are non-intuitive (Fig. 22). Thus the sliders control the parameters for an

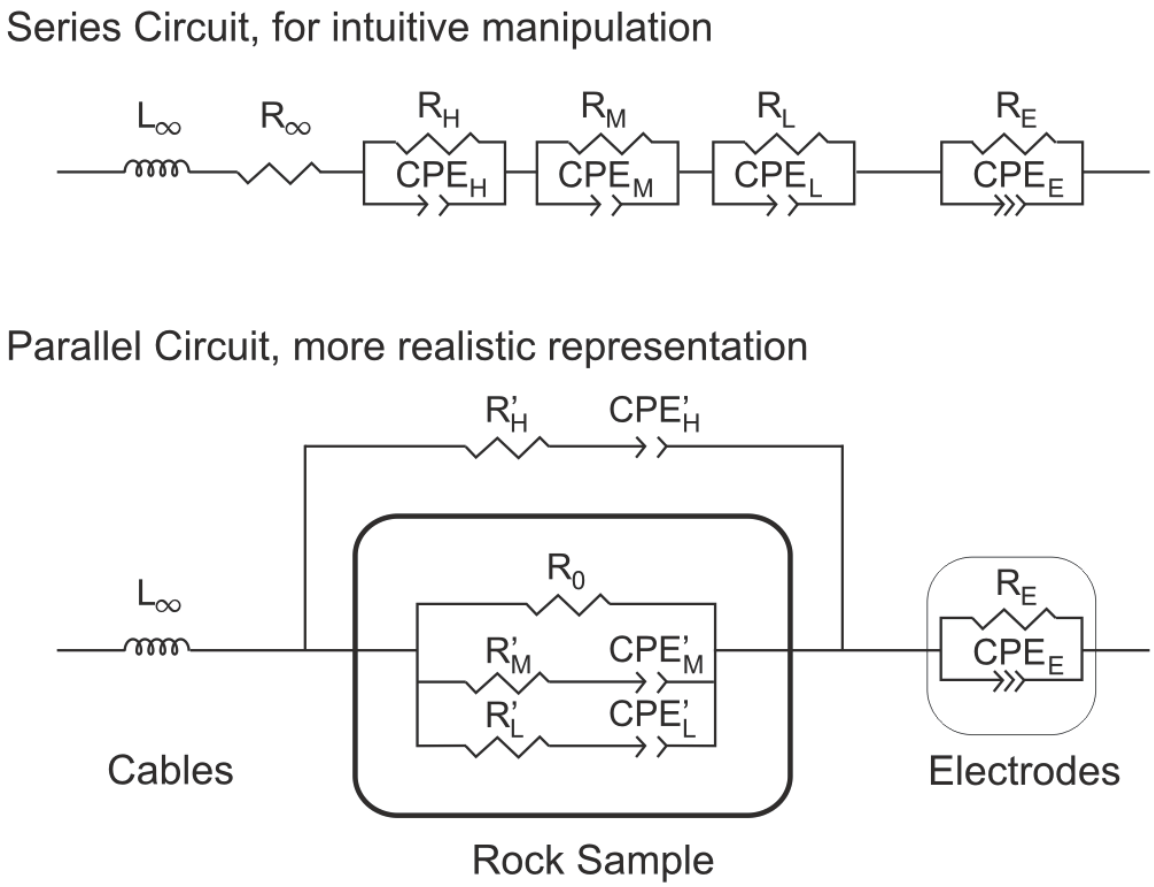

Figure 22: Equivalent circuits for analyzing rock impedance, including their measurement connections. The series circuit (top) is easier to manipulate, while the parallel circuit (bottom) is more realistic. Thus, the operator works with the analysis as if the equivalent circuit were in series form, while the program does calculations using the equivalent parallel form.

equivalent series circuit. The more realistic parallel circuit is used internally for the parameter optimization and for the interpretation of the petrophysical properties.

With reference to the series and parallel circuits of Figure 22, the following equations are used to transform the intuitive series circuit parameters (un-primed) to the more realistic parallel circuit parameters (with primes). The equations are approximate and are accurate only when there is no significant overlap in the relaxation time ranges between the parallel conduction mechanisms.

$$R'_0 = R_\infty + R_H + R_M + R_L \; . \quad [eq.9]$$

$$R'_H = R_\infty (R_\infty + R_H) / R_H \; . \quad [eq.10]$$

$$Q'_H = Q_H (R_H / (R_\infty + R_H))^2 \; . \quad [eq.11]$$

$$R'_M = (R_\infty + R_H) (R_\infty + R_H + R_M) / R_M \; . \quad [eq.12]$$

$$Q'_M = Q_M (R_M / (R_\infty + R_H + R_M))^2 \; . \quad [eq.13]$$

$$R'_L = (R_\infty + R_H + R_M) (R_\infty + R_H + R_M + R_L)/R_L \; . \quad [eq.14]$$

$$Q'_L = Q_M (R_L / (R_\infty + R_H + R_M + R_L))^2 \; . \quad [eq.15]$$

In practice, electrical impedance spectra are fit by manipulating the sliders to produce an approximate fit of the model to the observations, while ensuring that the 15 parameters are realistic. There are many local minima which the optimization procedure could locate, however most are nonsensical. It takes good physics understanding and experience to produce useful fits to the electrical impedance spectra.

Analysis of the electrical impedance spectra, and their relationships to lithology and complementary physical properties measurements, is still in its preliminary phase at the PPL. In Figure 23, the low electrical resistivity samples are dominantly of high magnetic susceptibility and high density, certainly caused by the concentration of sulphides which have high density, high electrical conductivity, and in the Great Bear Magmatic Zone from which these samples were taken, the mineralization is strongly associated with iron oxides.

In summary, a new method has been developed to analyze electrical impedance spectra of rock samples. The program ZARCFIT fits the EIS of the rock and the apparatus together with few assumptions. Although the individual parameters have significance concerning the mineralogy and permeability geometry of the sample, the main important parameters, resistivity and chargeability, are determined and compiled in the rock property database.

6. SUMMARY

The Paleomagnetism and Petrophysics Laboratory (PPL) at the Geophysical Survey of Canada has developed a standard set of measurements of physical properties of rocks. Rock property tables only provide the final results of density, magnetic properties and electrical properties. It is important for geologists and geophysicists who apply these data to understand the

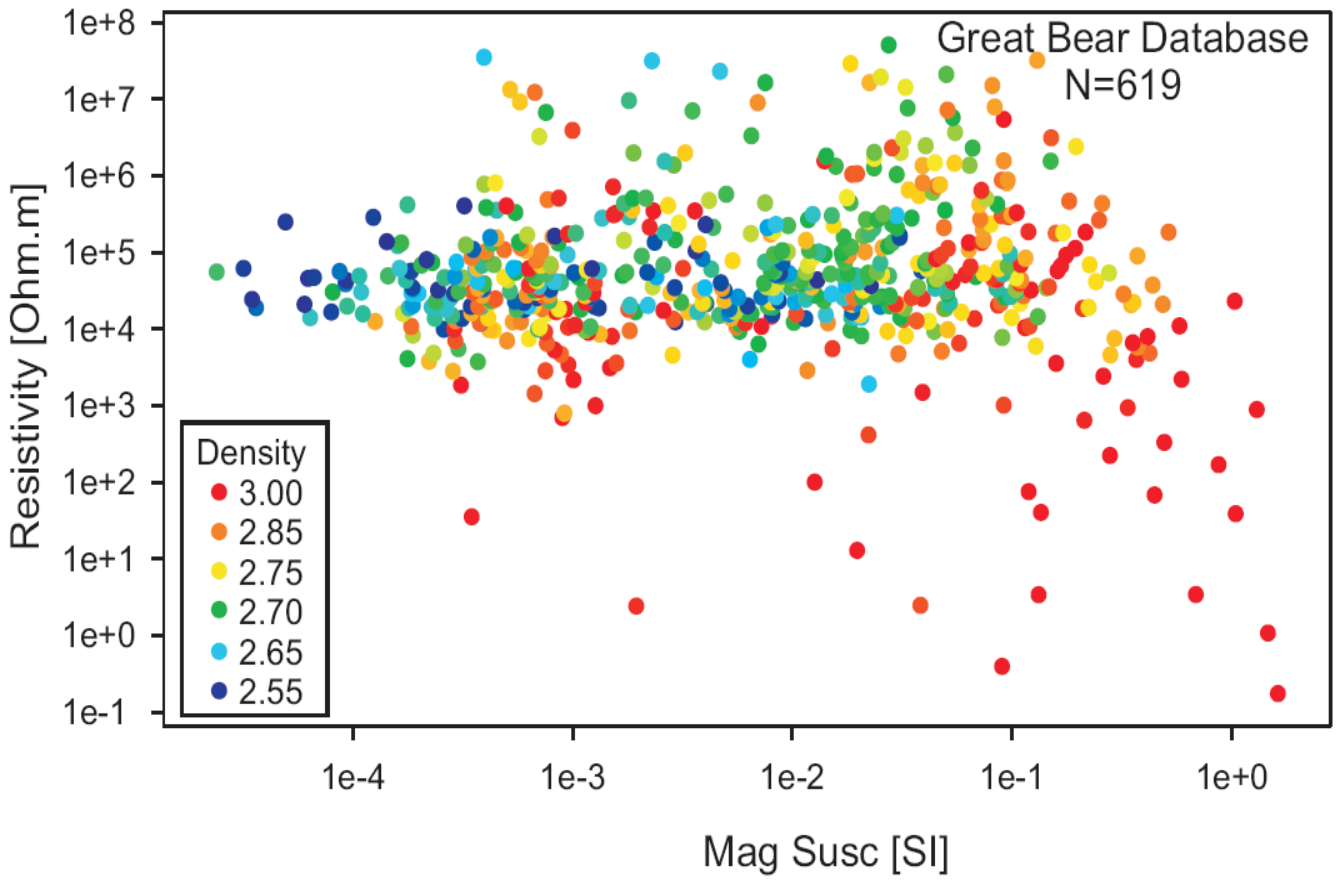

Figure 23: Relationship between magnetic susceptibility, density and electrical resistivity in the Great Bear-IOCG database.

methods used, their precision and their limits of applicability. This paper is designed as a single-reference documentation to simplify reporting and application of the rock properties database.

7. ACKNOWLEDGEMENTS

The development of the equipment, protocols, and documentation has taken place over many years and with the cooperation of many colleagues and students. I particularly thank Judith Baker, Kyle Bromma, Ken Cable, Devin Cowan, Mia Crewe, Darshan Crout, Nalin Dhillon, Tashi Drage, Najib El Goumi, Chris Galley, Damon Gilmour, Tark Hamilton, Jessica Holley, John Katsube, Marshall Kilduff, Erica Owen, Robert Rayner, Andrea Severide, Brendan Smithwick, Akhilla Srinivasan, Jennifer Tigner, Ashley Tkachyk, and Brad Vidal.

8. REFERENCES

Archie, G.E., 1942. The electrical resistivity log as an aid in determining some reservoir characteristics;. Petroleum Transactions of AIME, v. 146, p. 54–62.

Cole, K.S., and Cole, R.H., 1941. Dispersion and absorption in dielectrics - I Alternating current characteristics". Journal of Chemical Physics, v. 9, p. 341–352.

Day, R., Fuller, M., and Schmidt, V.A., 1977. Hysteresis properties of titanomagnetites: Grain size and composition dependence; Physics of the Earth and Planetary Intereriors, v. 13, p. 260–267.

Dunlop, D.J., 2002. Theory and application of the Day plot (Mrs/Ms versus Hcr/Hc) 1. Theoretical curves and tests using titanomagnetite data, Journal of Geophysical Research, v. 107, 2056, 22 p., doi:10.1029/2001JB000486.

Enkin, R.J., Baker, J., Nourgaliev, D., Iassonov, P., and Hamilton, T.S., 2007. Magnetic hysteresis parameters and Dayplot analysis to characterize diagenetic alteration in gas hydrate bearing sediments, Journal of Geophysical Research, v. 112, B06S90, doi:10.1029/ 2006JB004638.

Enkin, R.J., Vidal, B.S., Baker, J. and Struyk, N.M., 2008. Physical properties and paleomagnetic database for south-central British Columbia; in Geological Fieldwork 2007, B.C. Ministry of Energy Mines and Petroleum Resources, Paper 2008-1, p. 5-8.

Enkin, R.J., Cowan, D., Tigner J., Severide, A., Gilmour, D., Tkachyk, A., Kilduff, M., Vidal, B., and Baker, J., 2012, Physical property measurements at the GSC Paleomagnetism and Petrophysics Laboratory, including electric impedance spectrum methodology and analysis; Geological Survey of Canada, Open File 7227, 42 p.

Enkin, R.J., The Rock Physical Property Database of British Columbia, and the Distinct Signature of the Chilcotin Basalts, Canadian Journal of Earth Sciences, 51, 327-338, dx.doi.org/10.1139/cjes-2013-0159, 2014.

Enkin, R.J., Corriveau, L., and Hayward, N., Metasomatic alteration control of petrophysical properties in the Great Bear Magmatic Zone (Northwest Territories, Canada), Economic Geology, 111, 2073–2085, 2016

Heider, F., Zitzelsberger, A., and Fabian, K., 1996. Magnetic susceptibility and remanent coercive force in grown magnetite crystals from 0.1/xm to 6 mm; Physics of the Earth and Planetary Interiors, v. 93, p. 239-256.

Henkel, H., 1991. Petrophysical properties (density and magnetization) of rocks from the northern part of the Baltic Shield; Tectonophysics, v. 192, p. 1–19.

Henkel, H., 1994. Standard diagrams of magnetic properties and density – a tool for understanding magnetic petrology; Journal of Applied Geophysics, v. 32, p. 43–53.

Johnson, G.R., and Olhoeft G.R., 1984. Density of rocks and minerals; in Carmichael, R.S., ed., Handbook of physical properties of rocks; Volume III, CRC Press, Florida, p. 1-38.

Jolly, P., 1864. Eine Federwage zu exacten Wägungen; Sitzb. Akad. Wiss. München, v. 162, p. 166

Néel, L.,1955. Some theoretical aspects of rock magnetism; Advances in Physics, v. 4, no. 14, p. 191–243.

Parsons, S., McGaughey, J., Mitchinson, D., Phillips, N. and Lane, T.E., 2009. Development and application of a rock property database for British Columbia; in Geoscience B.C., Summary of Activities 2008, Geoscience B.C., Report 2009-1, p. 137–144.

Pelton, S. H., Ward, S. H., Hallof, P. G., Sill, W. R., and Nelson, P. H., 1978. Mineral discrimination and removal of inductive coupling with multifrequency IP; Geophysics, v. 43, p. 588-609.

Shimamura, K, Williams, S P., and Buller, G, 2008. GanFeld user guide: a map-based field data capture system for geologists; Geological Survey of Canada, Open File Report 5912; 90 p; doi:10.4095/226214.